ACS OMEGA

http://pubs.acs.org/journal/acsodf

Article

Synthesis of Silver Nanowires Using a Polyvinylpyrrolidone-Free Method with an *Alpinia zerumbet* Leaf Based on the Oriented Attachment Mechanism

Yanling Li, Ying Wang, Junqing Wu, Yingying Pan, Huangqing Ye,* and Xiping Zeng*

Cite This: *ACS Omega* 2023, 8, 2237−2242

Read Online

ACCESS | Metrics & More | Article Recommendations | Supporting Information

ABSTRACT: In this study, silver nanowires (AgNWs) were successfully synthesized by using a polyvinylpyrrolidone (PVP)-free hydrothermal method with an *Alpinia zerumbet* leaf chunk as a reducing agent and template. Meanwhile, the mechanism of biomass synthesis of AgNWs is also explored. The AgNWs have a diameter of ∼77 nm and a length of ∼10 μm. During the hydrothermal process, the biomass initially serves as a reducing agent to reduce silver ions. As the reaction proceeds, the biomass will form a pipe-shaped soft template by hydrothermal carbonization. Silver ions are adsorbed and reduced along the pipe-shaped soft templates to form silver nanorods, and adjacent nanorods are merged to AgNWs. Thus, AgNWs are grown along the pipeline soft template based on the oriented attachment mechanism. Inspired by this, the mechanism of the polyol method was further investigated. In the initial growth stage, AgNWs synthesized by the polyol method have a V-shaped notch. Therefore, AgNWs synthesized by the polyol method may also grow on the basis of the oriented attachment mechanism with PVP as a template.

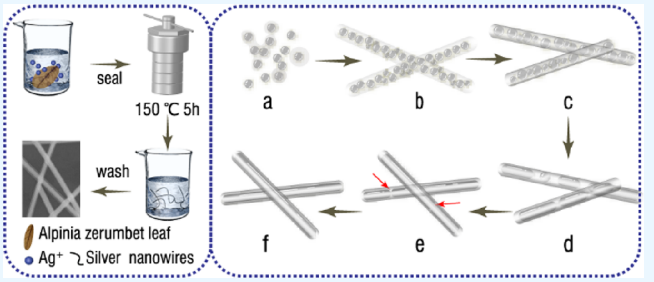

INTRODUCTION

Compared with bulk materials, nanomaterials have attracted considerable attention because of their excellent physical and chemical properties.[1−6] Silver nanowires (AgNWs), as a non-negligible metal nanowire material, have been extensively explored in electronics and photonics because of their high electron conductivity, optical transmittance, and tunable magnetic properties.[4,7,8]

AgNWs are usually synthesized by template,[9] electrochemical,[10] and wet chemical methods.[11] The wet chemical method has received attention because it allows easy adjustment of chemical reaction parameters to achieve products with high purity and specific morphologies.[12] In general, the wet chemical method includes polyol and hydrothermal methods.[13] For the polyol method, ethylene glycol (EG) is usually used as a solvent and reducing agent to dissolve and reduce silver ions. In addition, polyvinylpyrrolidone (PVP) is commonly believed to selectively combine on the Ag(100) crystal plane as a capping agent, which decreases the surface free energy and promotes the directional growth of silver atoms.[14] Therefore, facet-specific capping plays a crucial role in the final shape of silver.[15] The hydrothermal method uses water as a reaction and recrystallization medium, and it does not introduce other environmentally unfriendly materials. Also, the hydrothermal method is a simple operation with a possibility of mass production. Thus, the hydrothermal method is considered a green method for the synthesis of AgNWs.[14,16]

During the past decade, many biological systems have been proven to reduce inorganic metal ions.[17,18] For example, Lin et al.[19] reported that AgNWs with diameters of 50−60 nm were synthesized using broth of a *Cassia fistula* leaf. Flores-González et al.[20] synthesized AgNWs using commercial *Camellia sinensis* extracts and studied their antibacterial properties. Horta-Piñeres et al.[21] constructed AgNWs decorated with silver nanoparticles using *Mangifera indica* leaf extracts. However, these methods are cumbersome, and they usually require pretreatment of plants by drying, grinding, extracting, and filtering.[18,22]

Herein, we describe a PVP-free and environmentally friendly method to synthesize AgNWs. A piece of dried *Alpinia zerumbet* (*A. zerumbet*) leaf is directly placed into the reaction solution as a reducing agent and template without adding other chemical reagents. During the hydrothermal process, the biomass initially serves as a reducing agent to reduce silver ions and, then hydrothermal carbonization occurs to form a pipe-shaped soft template. Afterward, silver ions are adsorbed and reduced along the pipeline soft template. Thus, AgNWs grow

Received: October 8, 2022
Accepted: December 12, 2022
Published: January 4, 2023

https://doi.org/10.1021/acsomega.2c06481
ACS Omega 2023, 8, 2237−2242

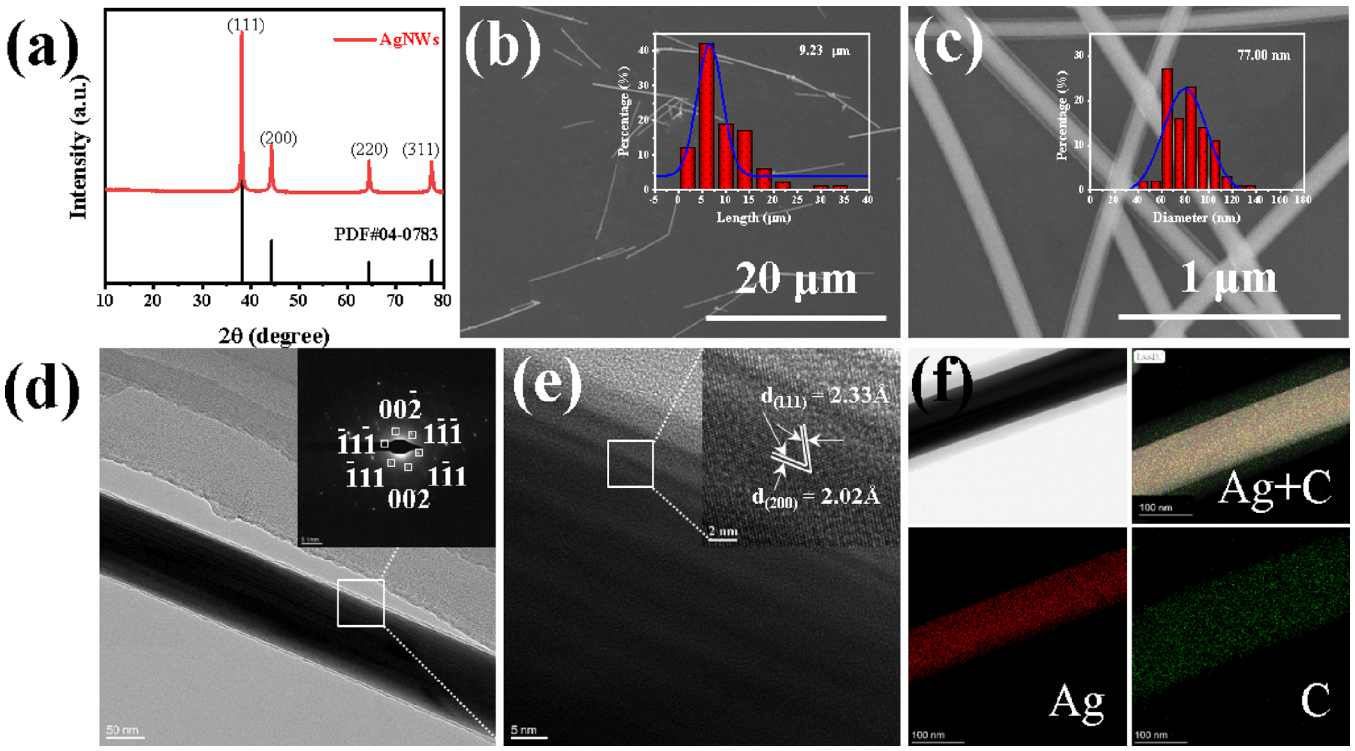

Figure 1. (a) XRD images of AgNWs synthesized with the biomass. (b, c) SEM images of AgNWs synthesized with the biomass; insets are the size distribution statistics of 100 silver nanowires. (d) TEM images of AgNWs synthesized with the biomass; the inset is the SAED image. (e) HRTEM pattern of AgNWs synthesized with the biomass; the inset is the partial enlargement image. (f) Element mapping.

in the pipeline soft template along a one-dimension orientation based on an oriented attachment (OA) mechanism. Compared with AgNWs synthesized using the traditional polyol method, those synthesized using the biomass exhibit excellent thermal stability at 200 °C. Composition analysis showed that the biomass was rich in tea polyphenols, lactose, and chloride ions. Subsequently, AgNWs were successfully synthesized using active ingredients under the same hydrothermal conditions. Furthermore, in the initial growth stage, AgNWs synthesized using the polyol method showed a V-shaped notch. Therefore, we speculate that, during the early stage of the polyol method, AgNWs may also grow on the basis of the OA mechanism with PVP as a template.

RESULTS AND DISCUSSION

Characterizations of AgNWs. The crystallographic structure of AgNWs synthesized with the biomass was obtained by XRD, and the XRD curves are shown in Figure 1a. Based on XRD, four strong diffraction peaks are clearly shown at (2θ) 38.05°, 44.31°, 64.43°, and 77.42°, which can be indexed as the face-centered cubic phase of silver (JCPDS card no. 04-0783). The lattice constant obtained from XRD was 4.084 Å, which is close to that previously reported (4.086 Å).[23,24] The morphology of AgNWs was initially observed by SEM (Figure 1b,c). Figure 1b shows that AgNWs dominated in the products, and a few silver nanoparticles piled up or adhered to AgNWs. Figure 1c indicates that after multiple washes, the surface of the AgNWs still has a uniform cladding layer. The distribution histogram of 100 AgNWs shows that the average diameter (inset of Figure 1b) and length (inset of Figure 1c) of AgNWs are ~77 nm and ~10 μm, respectively. The distribution histogram shows the AgNWs synthesized with the biomass with a narrow distribution of dimensions. In addition, we summarized the dimensions of AgNWs synthesized with the biomass in the literature in Table S1. Furthermore, TEM characterization showed that AgNWs had a core−shell structure (Figure 1d). The inset of Figure 1d is the selected area electron diffraction (SAED) pattern with the zone axis [110], and marked diffraction spots also indicate the silver crystal.[1,25,26] Based on Figure 1e and the inset, we determined interplanar distances of 0.233 and 0.202 nm, which correspond to (111) and (200) crystal planes of silver (JCPDS card no. 04-0783), so the AgNWs grow along the direction of (100). Element mapping (Figure 1f) displays the existence of Ag and C. Element C is sourced from the hydrothermal carbonization of sugar from the biomass.[27−30] Figure S2 shows the XPS spectrum, and the survey (Figure S2a) displays the peaks of Ag and C. Figure S2b is the high-resolution spectra of Ag 2d. The binding energies of 373.41 and 367.41 eV correspond to Ag $3d_{3/2}$ and Ag $3d_{5/2}$.[31] Figure S2c is the core-level spectra of C, which can be deconvoluted into four peaks. Four peaks located at 287.97, 285.41, 284.32, and 283.70 eV can be assigned to O−C═O, C−H, C−C, and C═C, respectively.[32]

We changed the biomass mass, reaction temperature, and ratio of $AgNO_3$ to biomass to explore the effect of different factors. Figure 2 shows the SEM image when the biomass quality is 0.50 g (Figure 2a), 0.75 g (Figure 2b), 1.00 g (Figure 2c), and 1.25 g (Figure 2d). The results indicate that when the biomass quality is too low (Figure 2a) or too high (Figure 2d), only silver nanoparticles can be observed because the quality of the biomass initially affects the content of the reducing agent and then the formation of pipe-shaped soft templates. When the biomass quality is too high, the coating is too thick, and when the biomass quality is too low, it is too low to form a pipe-shaped soft template, so neither can generate AgNWs in a

https://doi.org/10.1021/acsomega.2c06481
ACS Omega 2023, 8, 2237−2242

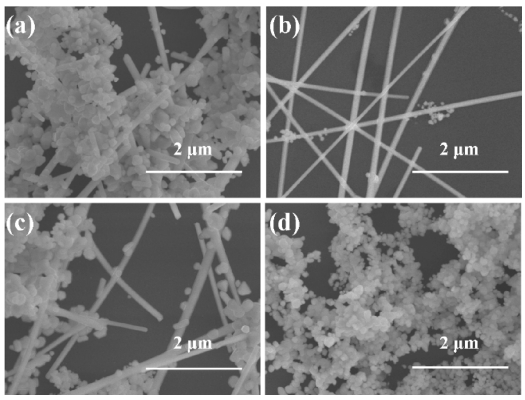

Figure 2. SEM images of AgNWs synthesized with a biomass quality of (a) 0.50 g, (b) 0.75 g, (c) 1.00 g, and (d) 1.25 g.

one-dimensional direction. A large amount and uniformity of AgNWs appeared when the biomass mass was 0.75 g, making it the suitable biomass quality. Different $AgNO_3$ and biomass ratios (Figure S3) exhibit similar results. The reaction temperature (Figure S4) can affect the release rate of active ingredients in leaves, thereby affecting the morphology of the final product.

Analysis of the Active Ingredients of the Biomass. In exploring the active ingredients of the biomass, the supernatant after the reaction was characterized through Fourier transform infrared spectroscopy (FTIR), ion chromatography (IC), and mass spectrometry (MS). Three vibration bands can be found in the region located at 1000−4000 cm^{-1} (Figure S5). FTIR spectra show very wide bands because the composition of the biomass is complex. The peak located at 3417.33 cm^{-1} can be assigned to the asymmetric vibration stretching of O−H, indicating the existence of hydroxyl groups.[19,33,34] The absorption spectra at 2122.86 cm^{-1} can be attributed to the vibrations caused by the scissoring and rocking of water.[35] The peak at 1650 cm^{-1} can be assigned to the stretching vibration of the −C═C− or C═O band.[33] An IC test (Figure S6) indicated the presence of chloride ions,[36] and the MS (Figure S7) result indicated the existence of lactose. Combined with the result obtained by Narusaka et al.,[37] that is, *A. zerumbet* leaf is rich in epicatechin, tea polyphenols (mainly composed of epicatechin), lactose, and chloride ions are effective components in the *A. zerumbet* leaf. The SEM results shown in Figure 3 indicate the synthesis of products only with tea polyphenols (Figure 3a) or lactose (Figure 3b) or tea polyphenols, lactose, and KCl (Figure 3c,d). Figure 3a shows that tea polyphenols exist as a reducing agent, and lactose (Figure 3b) will form a shell-like template; when they both exist, AgNWs can be observed (Figure 3c,d).

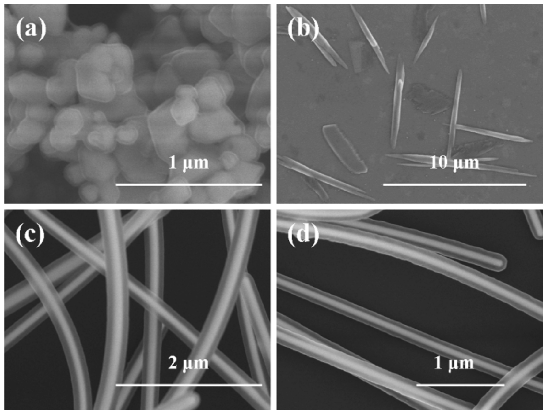

Figure 3. SEM images of the synthesis of (a) tea polyphenols, (b) lactose, and (c, d) tea polyphenols, lactose, and KCl.

Oriented Attachment Mechanism of AgNWs. In exploring the growth mechanism of AgNWs synthesized using biomass, AgNWs were sampled at different time periods during the reaction. Figure 4a shows the initial stage at 25 min wherein some small spherical silver nanoparticles were covered with a gauze-like substance. This finding indicates that free silver ions are initially adsorbed and then reduced to silver atoms by the biomass, thereby aggregating into silver nanoparticles covered by biomass. Afterward, the number of silver nanoparticles increases significantly and shows a regular arrangement (Figure 4b, 50 min). Prolonging the reaction time to 75 min (Figure 4c), the average particle size of silver nanoparticles increases, and the biomass layer is tightly wrapped around the silver nanoparticles. During this time, the organic layer is gradually hydrothermally carbonized as a pipe-shaped soft template (inset image of Figure 4c). When the reaction time reaches 100 min (Figure 4d), SEM images show a pipe-shaped soft template approximately 100 nm in width. A small amount of silver nanoparticles is adsorbed on the pipeline soft template. Moreover, in the pipe-shaped soft template, discontinuous silver nanorods can be observed with a breadth of ∼50 nm (pointing with a white arrow). In the inset of Figure 4d (TEM), the continuous conduit template and discontinuous nanorods can also be observed. The pipeline soft template induced the growth of AgNWs along one-dimensional orientations; therefore, PVP is not necessary. When the reaction time reaches 150 min (Figure 4e), such discontinuous nanorods merged to form AgNWs with a V-shape notch (pointing with a white arrow). Finally, when the reaction time reaches 300 min (Figure 4f), AgNWs with a well-defined shape are obtained.

The classical nanocrystal growth theory refers to Ostwald ripening in which the smaller nanoparticles are gradually consumed by the larger ones.[19,38] In nanoscale systems, another vital mechanism, namely, "oriented attachment", was found, where nanoparticles with common crystallographic orientations directly combine to form larger ones.[38] Peng et al.[39] reported that, after removing PVP on crystal facets, AgNWs will orientationally self-attach to form longer AgNWs. In this work, discontinuous silver nanorods appear in the pipeline soft template during the middle stage of the reaction, and they are not covered with a PVP layer. Lin et al.[19] observed a similar phenomenon using broth of a *Cassia fistula* leaf to prepare AgNWs in which, rather than forming through a point-initiated vectorial growth, the AgNWs formed by the recrystallization of adjacent nanoparticles in a linear aggregation. In this paper, silver ions are first reduced to silver atoms, which are aggregated into silver nanoparticles. Small silver nanoparticles grow up through Ostwald ripening. Afterward, nanoparticles met and then adhered to form short silver nanorods by van der Waals forces.[40] Finally, the discontinuous silver nanorods merge with adjacent nanorods to AgNWs in the limitation of the pipe-shaped soft templates. Thus, AgNWs synthesized using the biomass are grown through a template-dependent OA mechanism.

AgNWs are also synthesized using the polyol method to explore the growth mechanism. AgNWs cannot be synthesized when the PVP molecular weight is low at 8000. The PVP_{8000}

https://doi.org/10.1021/acsomega.2c06481
ACS Omega 2023, 8, 2237−2242

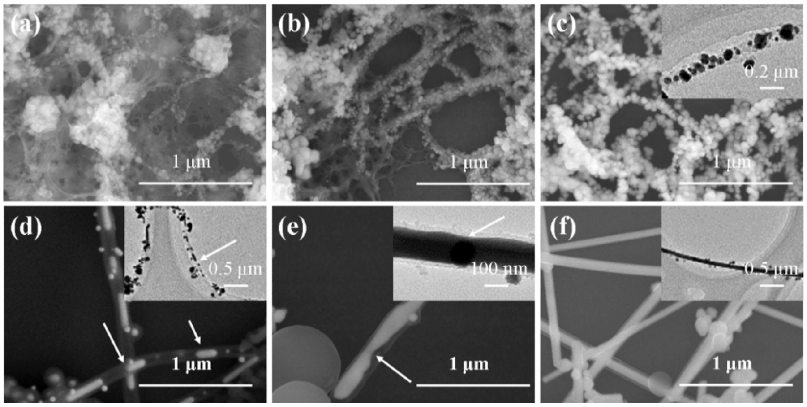

Figure 4. SEM images of AgNWs synthesized for (a) 25 min, (b) 50 min, (c) 75 min, (d) 100 min, (e) 150 min, and (f) 300 min. Inset (c–f) is the TEM images.

chain length is only ~18 nm; thus, the PVP template cannot collect enough silver ions to form AgNWs. In addition, AgNWs do not appear until the PVP molecular weight reaches 29,000, and a positive correlation is observed between the length of AgNWs and PVP molecular weights (Figure 5a). Details of

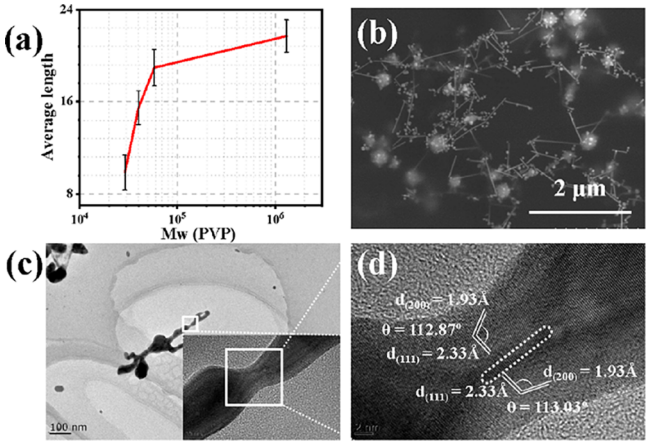

Figure 5. (a) Curves between the length of AgNWs and the different molecular weights of PVP. (b) SEM image of AgNWs synthesized with polyol. (c, d) TEM image of AgNWs synthesized with polyol.

AgNWs synthesized with different PVP molecular weights are shown in Figure S8. When the PVP molecular weight is 1,300,000, AgNWs were sampled in the early stage of the reaction (about 10 min after adding Ag^+). The SEM images are shown in Figure 5b, which are dominantly short AgNWs with a length of 1 μm. Figure 5c shows the TEM image of AgNWs with a V-shaped notch. As shown in Figure 5d, the plane spacing values of 0.233 and 0.193 nm are consistent with the (111) and (200) facets of silver. However, the crystal plane angle (~113°) of (111) and ($\bar{2}$00) is smaller than the theoretical value of 125°, which may be attributed to the misorientation when OA forms a twin boundary (highlighted with a dashed circle).[39] Kuo et al.[41] also reported that AgNWs are grown by self-assembly with nanorods and spheres. Therefore, the AgNWs synthesized by the polyol method may also grow on the basis of the OA mechanism by PVP as a template during the early stage.

Thermal Stability. Figure 6a,b shows the SEM image of AgNWs with similar diameters synthesized with the biomass and EG. The method synthesis of AgNWs by EG is in

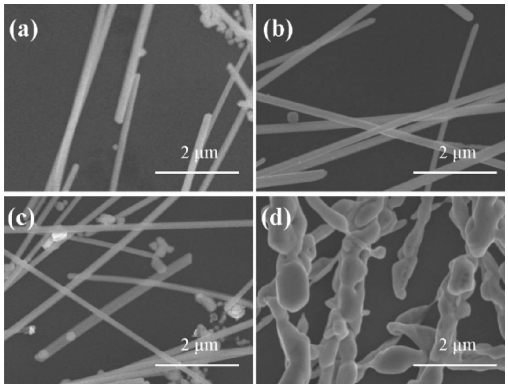

Figure 6. SEM images of AgNWs synthesized with (a) biomass and (b) ethylene glycol. SEM image of AgNWs treated with (c) the biomass and (d) ethylene glycol at 200 °C for 4 h.

accordance with Zhang et al.'s[42] work. After heating at 200 °C for 4 h, AgNWs synthesized with the biomass basically maintain their original form (Figure 6c), and the control group AgNWs are completely invalid (Figure 6d). The improvement of thermal stability may be attributed to the biomass carbonization layer. This provides a possibility for the development of high-thermal-stability, flexible AgNW transparent conductive films.

CONCLUSIONS

We have provided a PVP-free and environmentally friendly method to synthesize AgNWs using an *A. zerumbet* leaf as a reducing agent and template. The AgNWs have a diameter of ~77 nm and a length of ~10 μm. The results of our study show that biomass is rich in tea polyphenols, lactose, and chloride ions and AgNWs are grown on the basis of the OA mechanism. Exploring further, in the early stage of the polyol method, AgNWs with a V-shaped notch are found, and therefore, AgNWs synthesized by the polyol method may also grow on the basis of the OA mechanism by PVP as a template. In addition, AgNWs exhibit excellent thermal stability at 200 °C. This provides a possibility for the development of high-thermal-stability, flexible AgNW transparent conductive films.

MATERIALS AND METHODS

Materials. Silver nitrate ($AgNO_3$, ≥99.0%, AR, Sinopharm Group Chemical Reagent Co., Ltd., China), EG ($C_2H_6O_2$, ≥98.0%, AR, Aladdin), potassium chloride (KCl, ≥99.5%, AR,

https://doi.org/10.1021/acsomega.2c06481
ACS Omega 2023, 8, 2237−2242

Macklin), and PVP ($(C_6H_9NO)_n$; M_w = 8000, 29,000, 40,000, 58,000, and 1,300,000; ≥99.0%, AR, Aladdin) were used in this study. An *A. zerumbet* leaf was collected in Shenzhen, Guangdong Province, China. All the chemical agents were used without further purification, and deionized water was used with 18.2 MΩ cm.

Preparation of AgNWs Using Biomass and Active Ingredients. The *A. zerumbet* leaf (large green leaves) was cut into ∼5 cm squares and cleaned with deionized water to remove surface dust then dried at 60 °C for a week to dehydrate it completely. First, 0.5 g of $AgNO_3$ was dissolved in 35 mL of deionized water with ultrasonic cleaning. Then, 0.75 g of dry *A. zerumbet* leaf chunks was added directly to the abovementioned $AgNO_3$ solution. Finally, the mixture was carefully transferred into a 50 mL Teflon-lined autoclave and heated at 150 °C for 5 h. The precipitate was washed with water and ethanol and preserved in ethanol solution.

AgNWs were also synthesized by using active ingredients. $AgNO_3$ (0.25 g) was dissolved into 35 mL of deionized water with ultrasonic cleaning and added with tea polyphenols (40 mg), lactose (90 mg), and KCl (50 mg). The rest of the operations are the same as previously mentioned.

Preparation of AgNWs by EG. An amount of 0.24 g of KCl and 5 g of PVP were completely dissolved in 500 mL of EG at 140 °C with magnetic stirring. Ten milliliters of 1.2 M $AgNO_3$ solution was gradually added to the abovementioned solution. The reaction lasted for 2 h until the liquid changed to silver gray. Moreover, the precipitate was washed with water and ethanol and preserved in ethanol solution.

Characterization. The AgNWs prepared using the biomass were dried in an oven at 60 °C, and the powder was used for the following characterization. The elemental composition and structure of the product were collected using X-ray photoelectron spectroscopy (XPS, Thermo Scientific K-Alpha) and X-ray diffraction (XRD, Rigaku Miniflex 600). Surface morphologies were obtained by field-emission scanning electron microscopy (FESEM, HITACHI Regulus 8100) and high-resolution transmission electron microscopy (HRTEM, FEI Talos F200X G2). The surface elemental distribution of the specimen was characterized by mapping. In order to obtain information on the effective components of the biomass, Fourier transform infrared spectroscopy (FTIR, Nicolet iS 10) was done.

To explore the active ingredients of the biomass, the supernatant after the reaction was filtered with a 0.45 um strainer. The supernatant was used to conduct mass spectrometry (MS, Bruker solariX FT-MS). After the supernatant was diluted 5000 times, it was subjected to ion chromatography (IC, ICS-1100).

■ ASSOCIATED CONTENT

Supporting Information

The Supporting Information is available free of charge at https://pubs.acs.org/doi/10.1021/acsomega.2c06481.

Summary table of the dimensions of AgNWs synthesized by other types of biomass, XPS spectrum, SEM diagram of samples with different synthesis parameters, and characterization data related to active ingredients of the biomass (PDF)

■ AUTHOR INFORMATION

Corresponding Authors

Huangqing Ye − *International Collaborative Laboratory of 2D Materials for Optoelectronics Science and Technology of the Ministry of Education, Institute of Microscale Optoelectronics, Shenzhen University, Shenzhen, Guangdong 518060, China*; Email: beyondye88@gmail.com

Xiping Zeng − *Research and Develop Center, Shenzhen Huake-Tek Co., Ltd., Shenzhen, Guangdong 518116, China*; orcid.org/0000-0003-4002-347X; Email: xzengad@connect.ust.hk

Authors

Yanling Li − *Research and Develop Center, Shenzhen Huake-Tek Co., Ltd., Shenzhen, Guangdong 518116, China*

Ying Wang − *Research and Develop Center, Shenzhen Huake-Tek Co., Ltd., Shenzhen, Guangdong 518116, China*

Junqing Wu − *Research and Develop Center, Shenzhen Huake-Tek Co., Ltd., Shenzhen, Guangdong 518116, China*

Yingying Pan − *Research and Develop Center, Shenzhen Huake-Tek Co., Ltd., Shenzhen, Guangdong 518116, China*

Complete contact information is available at: https://pubs.acs.org/10.1021/acsomega.2c06481

Notes

The authors declare no competing financial interest.

■ ACKNOWLEDGMENTS

This work was supported by the Natural Science Foundation of China (grant nos. 61705137 and 52002250), the Science and Technology Project of Shenzhen (no. KQJSCX20180328093614762), and the Shenzhen Peacock Plan (no. KQTD2016022614361432). The author also acknowledges the characterization assistance of Shiyanjia Lab (www.shiyanjia.com) for the XPS and TEM.

■ REFERENCES

(1) Gao, Y.; Song, L.; Jiang, P.; Liu, L. F.; Yan, X. Q.; Zhou, Z. P.; Liu, D. F.; Wang, J. X.; Yuan, H. J.; Zhang, Z. X.; Zhao, X. W.; Dou, X. Y.; Zhou, W. Y.; Wang, G.; Xie, S. S.; Chen, H. Y.; Li, J. Q. Silver nanowires with five-fold symmetric cross-section. *J. Cryst. Growth* **2005**, *276*, 606−612.

(2) Vijayaraghavan, K.; Nalini, S. P.; Prakash, N. U.; Madhankumar, D. One step green synthesis of silver nano/microparticles using extracts of Trachyspermum ammi and Papaver somniferum. *Colloids Surf., B* **2012**, *94*, 114−117.

(3) Zhang, P.; Wyman, I.; Hu, J.; Lin, S.; Zhong, Z.; Tu, Y.; Huang, Z.; Wei, Y. Silver nanowires: Synthesis technologies, growth mechanism and multifunctional applications. *Mater. Sci. Eng., B* **2017**, *223*, 1−23.

(4) Fahad, S.; Yu, H.; Wang, L.; Zain Ul, A.; Haroon, M.; Ullah, R. S.; Nazir, A.; Naveed, K.-U.-R.; Elshaarani, T.; Khan, A. Recent progress in the synthesis of silver nanowires and their role as conducting materials. *J. Mater. Sci.* **2018**, *54*, 997−1035.

(5) Han, J.; Yang, J.; Gao, W.; Bai, H. Ice-Templated, Large-Area Silver Nanowire Pattern for Flexible Transparent Electrode. *Adv. Funct. Mater.* **2021**, *31*, No. 2010155.

(6) Ye, H.; Zhuang, G.; Pan, Y.; Wang, H.; Li, Y.; Lin, Y.; Wang, Y.; Zeng, X. Controllable synthesis of silver nanowires via an organic cation-mediated polyol method and their application as transparent electrode for touch screen. *Nano Sel.* **2022**, 1−1313.

(7) Kawamura, G.; Muto, H.; Matsuda, A. Hard template synthesis of metal nanowires. *Front. Chem.* **2014**, *2*, 104−108.

(8) Xiang, X.-Z.; Gong, W.-Y.; Kuang, M.-S.; Wang, L. Progress in application and preparation of silver nanowires. *Rare Met.* **2016**, *35*, 289−298.
(9) Lin, Y.-H.; Chen, K.-T.; Ho, J.-R. Rapid Fabrication of Silver Nanowires through Photoreduction of Silver Nitrate from an Anodic-Aluminum-Oxide Template. *Jpn. J. Appl. Phys.* **2011**, *50*, No. 065002.
(10) Mazur, M. Electrochemically prepared silver nanoflakes and nanowires. *Electrochem. Commun.* **2004**, *6*, 400−403.
(11) Wang, Z.; Liu, J.; Chen, X.; Wan, J.; Qian, Y. A simple hydrothermal route to large-scale synthesis of uniform silver nanowires. *Chem. − Eur. J.* **2004**, *11*, 160−163.
(12) Tan, D.; Jiang, C.; Li, Q.; Bi, S.; Song, J. Silver nanowire networks with preparations and applications: a review. *J. Mater. Sci.: Mater. Electron.* **2020**, *31*, 15669−15696.
(13) Tetsumoto, T.; Gotoh, Y.; Ishiwatari, T. Mechanistic studies on the formation of silver nanowires by a hydrothermal method. *J. Colloid Interface Sci.* **2011**, *362*, 267−273.
(14) Zhu, Y.; Deng, Y.; Yi, P.; Peng, L.; Lai, X.; Lin, Z. Flexible Transparent Electrodes Based on Silver Nanowires: Material Synthesis, Fabrication, Performance, and Applications. *Adv. Mater. Technol* **2019**, *4*, No. 1900413.
(15) Xia, X.; Zeng, J.; Zhang, Q.; Moran, C. H.; Xia, Y. Recent Developments in Shape-Controlled Synthesis of Silver Nanocrystals. *J. Phys. Chem. C* **2012**, *116*, 21647−21656.
(16) Li, W.; Zhang, H.; Shi, S.; Xu, J.; Qin, X.; He, Q.; Yang, K.; Dai, W.; Liu, G.; Zhou, Q.; Yu, H.; Silva, S. R. P.; Fahlman, M. Recent progress in silver nanowire networks for flexible organic electronics. *J. Mater. Chem. C* **2020**, *8*, 4636−4674.
(17) Makarov, V. V.; Sinitsyna, O. V.; Makarova, S. S.; Yaminsky, I. V.; Taliansky, M. E.; Kalinina, N. O. "Green" nanotechnologies synthesis of metal nanoparticles using plants. *Acta Naturae* **2014**, *6*, 35−44.
(18) Rolim, W. R.; Pelegrino, M. T.; de Araújo Lima, B.; Ferraz, L. S.; Costa, F. N.; Bernardes, J. S.; Rodigues, T.; Brocchi, M.; Seabra, A. B. Green tea extract mediated biogenic synthesis of silver nanoparticles: Characterization, cytotoxicity evaluation and antibacterial activity. *Appl. Surf. Sci.* **2019**, *463*, 66−74.
(19) Lin, L.; Wang, W.; Huang, J.; Li, Q.; Sun, D.; Yang, X.; Wang, H.; He, N.; Wang, Y. Nature factory of silver nanowires: Plant-mediated synthesis using broth of Cassia fistula leaf. *Chem. Eng. J.* **2010**, *162*, 852−858.
(20) Flores-González, M.; Talavera-Rojas, M.; Soriano-Vargas, E.; Rodríguez-González, V. Practical mediated-assembly synthesis of silver nanowires using commercial Camellia sinensis extracts and their antibacterial properties. *New J. Chem.* **2018**, *42*, 2133−2139.
(21) Horta-Piñeres, S.; Britto Hurtado, R.; Avila-Padilla, D.; Cortez-Valadez, M.; Flores-Lòpez, N. S.; Flores-Acosta, M. Silver nanoparticle-decorated silver nanowires: a nanocomposite via green synthesis. *Appl. Phys. A: Mater. Sci. Process.* **2020**, *126*, 15−25.
(22) Lü, F.; Gao, Y.; Huang, J.; Sun, D.; Li, Q. Roles of Biomolecules in the Biosynthesis of Silver Nanoparticles: Case of Gardenia jasminoides Extract. *Chin. J. Chem. Eng.* **2014**, *22*, 706−712.
(23) Sun, Y.; Yin, Y.; Mayers, B. T.; Herricks, T.; Xia, Y. Uniform silver nanowires synthesis by reducing $AgNO_3$ with ethylene glycol in the presence of seeds and poly (vinyl pyrrolidone). *Chem. Mater.* **2002**, *14*, 4736−4745.
(24) Zhao, W.; Wang, S.-S.; Cao, H.-T.; Xie, L.-H.; Hong, C.-S.; Jin, L.-Z.; Yu, M.-N.; Zhang, H.; Zhang, Z.-Y.; Huang, L.-H.; Huang, W. An eco-friendly water-assisted polyol method to enhance the aspect ratio of silver nanowires. *RSC Adv.* **2019**, *9*, 1933−1938.
(25) Graff, A.; Wagner, D.; Ditlbacher, H.; Kreibig, U. Silver nanowires. *Eur. Phys. J. D* **2005**, *34*, 263−269.
(26) Zheng, X.; Zhu, L.; Yan, A.; Wang, X.; Xie, Y. Controlling synthesis of silver nanowires and dendrites in mixed surfactant solutions. *J. Colloid Interface Sci.* **2003**, *268*, 357−361.
(27) Sun, X. M.; Li, Y. D. Cylindrical Silver Nanowires: Preparation Structure, and Optical Properties. *Adv. Mater.* **2005**, *17*, 2626−2630.
(28) Shen, Y. A review on hydrothermal carbonization of biomass and plastic wastes to energy products. *Biomass Bioenergy* **2020**, *134*, No. 105479.
(29) Sun, X.; Li, Y. Colloidal Carbon Spheres and Their Core/Shell Structures with Noble-Metal Nanoparticles. *Am. Ethnol.* **2004**, *116*, 607−611.
(30) Ye, H.; Chen, J.; Hu, Y.; Li, G.; Fu, X. Z.; Zhu, P.; Sun, R.; Wong, C. P. One-pot synthesis of two-dimensional multilayered graphitic carbon nanosheets by low-temperature hydrothermal carbonization using the in situ formed copper as a template and catalyst. *Chem. Commun.* **2020**, *56*, 11645−11648.
(31) Chastain, J.; King, Jr, R. C. *Handbook of X-ray photoelectron spectroscopy*, Perkin-Elmer Corporation 1992, *40*, 221.
(32) Chen, X.; Wang, X.; Fang, D. A review on C1s XPS-spectra for some kinds of carbon materials. *Fullerenes, Nanotubes, Carbon Nanostruct.* **2020**, *28*, 1048−1058.
(33) Movasaghi, Z.; Rehman, S.; Ur Rehman, D. I. Fourier Transform Infrared (FTIR) Spectroscopy of Biological Tissues. *Appl. Spectrosc. Rev.* **2008**, *43*, 134−179.
(34) Dovbeshko, G. I.; Gridina, N. Y.; Kruglova, E. B.; Pashchuk, O. P. FTIR spectroscopy studies of nucleic acid damage. *Talanta* **2000**, *53*, 233−246.
(35) Dankar, I.; Haddarah, A.; Omar, F. E. L.; Pujola, M.; Sepulcre, F. Characterization of food additive-potato starch complexes by FTIR and X-ray diffraction. *Food Chem.* **2018**, *260*, 7−12.
(36) Amin, M.; Lim, L. W. Ion chromatographic method for the simultaneous determination of anions and cations in firecrackers and matches samples as known potential explosives. *ALCHEY Jurnal Penelitian Kimia* **2019**, *15*, 138−149.
(37) Morimoto, H.; Hatanaka, T.; Narusaka, M.; Narusaka, Y. Molecular investigation of proanthocyanidin from Alpinia zerumbet against the influenza A virus. *Fitoterapia* **2022**, *158*, No. 105141.
(38) Zhang, J.; Huang, F.; Lin, Z. Progress of nanocrystalline growth kinetics based on oriented attachment. *Nanoscale* **2010**, *2*, 18−34.
(39) Peng, P.; Liu, L.; Gerlich, A. P.; Hu, A.; Zhou, Y. N. Self-Oriented Nanojoining of Silver Nanowires via Surface Selective Activation. *Part. Part. Syst. Charact.* **2013**, *30*, 420−426.
(40) Zhao, Q.; Qiu, J.; Zhao, C.; Hou, L.; Zhu, C. Synthesis and Formation Mechanism of Silver Nanowires by a Templateless and Seedless Method. *Chem. Lett.* **2005**, *34*, 30−31.
(41) Kuo, C. L.; Hwang, K. C. Nitrate ion promoted formation of Ag nanowires in polyol processes: a new nanowire growth mechanism. *Langmuir* **2012**, *28*, 3722−3729.
(42) Zhang, Z.; Wu, Y.; Wang, Z.; Zhang, X.; Zhao, Y.; Sun, L. Electrospinning of Ag Nanowires/polyvinyl alcohol hybrid nanofibers for their antibacterial properties. *Mater. Sci. Eng., C* **2017**, *78*, 706−714.

https://doi.org/10.1021/acsomega.2c06481
ACS Omega 2023, 8, 2237−2242